On the selection of Johnson-Cook constitutive model parameters for Ti-6Al-4V using three types of numerical models of orthogonal cutting

Yancheng Zhang[a,*], J.C. Outeiro[b], Tarek Mabrouki[c]

[a] *University of Lyon, CNRS, INSA-Lyon, LaMCoS UMR 5259, Lyon, France*
[b] *Arts et Métiers ParisTech, LaBoMaP, Rue Porte de Paris, 71250, Cluny, France*
[c] *University of Tunis El-Manar, ENIT, BP-37, Le Belvédère 1002, Tunis, Tunisie*

* Corresponding author. Tel.: + 33 4 72 43 74 67; fax: + 33 4 78 89 09 80. *E-mail address:* yancheng.zhang@insa-lyon.fr.

Abstract

Johnson-Cook constitutive model is still the most used model in metal cutting simulation, although several drawbacks reported in the literature. A high number of Johnson-Cook model parameters can be found in the literature for the same work material. One question that may arise is "What is the most suitable set of Johnson-Cook model parameters for a given material?". The present paper puts in evidence some issues related with the selection of these parameters from the literature.
In this contribution, two sets of Johnson-Cook model parameters for Ti-6A-4V are evaluated, using three types of metal cutting models. These models are based on three different formulations: Lagrangian, Arbitrary Eulerian-Lagrangian (ALE) and Couple Lagrangian-Eulerian (CEL). This evaluation is based on the comparison between measured and predicted chip geometry, chip compression ratio, forces, plastic deformation and temperature distributions.

Keywords: Modelling; Finite element method (FEM); Cutting; Material removal

1. Introduction

Modelling and simulation are today exciting approaches for analyzing and investigating metal cutting process. Despite, the advances in the development in architecture of machine tools, their monitoring and process controlling, many scientists and industrials, in different research laboratories, are yet working on optimizing the machining process. For example, they are developing and/or using various models to predict the machining performance in terms of cutting forces, temperatures, hardness, microstructural and phase changes, residual stresses, tool-wear, part distortion, surface roughness, chip breaking/breakability, process dynamics, stability of machining operations, etc. [1–7]. So, a large amount of the research work dedicated to the machining process, are mainly focused on the understanding improvement of the tool-material interaction. The effectiveness of these models to predict the machining performance has been questionable, because of the poor representation of the actual metal cutting process yielding to inadequate quality and accuracy of the used input data [7]. The thermo-mechanical behavior of the work material is one, among others, which can be considered as critical input data. As shown by Astakhov [8], the principal difference that exists between machining and all other metal forming processes is the physical separation of the layer being removed (in the form of chips) from the rest of the workpiece. The process of physical separation of a solid body into two or more parts is based on fracture phenomenon. Consequently, machining has to be treated as the purposeful fracture of the layer being removed. From this context, a proper modeling of work material in machining should take into account not only the determination of the material flow stress under similar conditions as those observed in machining, but also under which conditions the fracture would occurs and how to model it adequately.

Among the literature published [9] on the topic of modeling machining operations based on FE method, it can be underlined that the Lagrangian approach is widely used to model the movement description inside cutting model [5]. Nevertheless, this approach introduces model mesh distortion, which can be avoided by adopting Eulerian and Arbitrary Lagrangian - Eulerian (ALE) approaches. The latter can be employed at the cost of non-real chip and calculation time compared to Lagrangian model. For the coupled Eulerian-Lagrangian (CEL) method in items of coupling of Eulerian workpiece and Lagrangian tool, the mesh is fixed in space and material flows through the element faces allowing large strains without causing mesh distortion problems [10].

The present paper emphasizes on the selection of the most suitable Johnson-Cook (J-C) constitutive model parameters for the Ti-6Al-4V. Two sets of parameters were used in three types of orthogonal cutting models, corresponding to three different numerical formulations: Lagrangian, ALE and CEL. The aim is to identify the most suitable set of Johnson-Cook (J-C) model parameters that produce the best fit between predicted and measured results concerning to: chip geometry, chip compression ratio, forces (cutting force and thrust forces) and the distributions of temperature and equivalent plastic strain.

2. Johnson-Cook constitutive model and numerical formulations

2.1. Johnson-Cook constitutive model

Several constitutive models are used today in metal cutting simulations. However, the Johnson-Cook (J-C) phenomenological constitutive model [11] is probably the most used and available in most of the commercial FE codes. This model considers the separated effects of strain hardening, strain-rate (viscosity) and thermal softening. It is usually represented by the following equation:

$$\bar{\sigma} = \underbrace{\left(A + B\bar{\varepsilon}^{n}\right)}_{\text{Strain hardening effect}} \underbrace{\left[1 + C\,ln\left(\frac{\dot{\bar{\varepsilon}}}{\dot{\bar{\varepsilon}}_0}\right)\right]}_{\text{Strain-rate (viscosity) effect}} \underbrace{\left[1 - \left(\frac{T - T_{room}}{T_m - T_{room}}\right)^{m}\right]}_{\text{Thermal softening effect}} \quad (1)$$

where $\bar{\sigma}$ is the equivalent plastic stress (MPa), $\bar{\varepsilon}$ is the equivalent plastic strain, $\dot{\bar{\varepsilon}}$ is the equivalent plastic strain rate (s^{-1}), $\dot{\bar{\varepsilon}}_0$ is the reference equivalent plastic strain rate (s^{-1}), T is the temperature (°C), T_m is the melting temperature of the work material (°C) and T_{room} is the room temperature (°C). *A, B, C, m* and *n* are material parameters, which are determined based on the flow stress data obtained from mechanical tests.

As mentioned by Guo and Horstemeyer [12], although this model is easy to apply and can describe the general response of material deformation, it's deficient to reflect the static and dynamic recovery, and the effects of load path and strain-rate history in large deformation processes, such is the case of metal cutting process. These effects are fundamental to proper modeling the surface integrity of machined components, including the residual stress distribution [12, 13]. Moreover, presuming that no external heat source is added to the cutting process, the term on thermal softening of the J-C constitutive model (see Eq. 1) is not necessary. In fact, the heat generated under high strain-rates accelerates the temperature rise and creates adiabatic localized regions. Thus, the strain hardening measured in high rate material testing may include the thermal softening effects as well [14]. Another issue is related to the determination of the (J-C) material parameters from mechanical tests. The split Hopkinson pressure bar (*SHPB*) [15] is largely used to determine the work material flow stress under high strain-rates, frequently encountered to metal cutting. Unfortunately, the SHPB has some drawbacks that can compromise the validity of the results, including the oscillations that flow stress exhibits particularly at low strains [16]. Moreover, the flow stress depends on the strain path [12], which accords to Silva et al. [17], is different from that found in metal cutting. In order to improve the ability to J-C model to predict the flow stress in machining, some researchers have modified the J-C constitutive model. For example, Calamaz et al. [18] modified the J-C flow stress model by considering the strain softening effect on flow stress. Similar to Calamaz et al., Sima and Ozel [19] also modified the J-C model by considering the temperature depended strain softening. To get the same effect, fracture energy-based damage evolution is also proposed by Mabrouki et al. [5] to accomplish material degradation and get segmented chip morphology.

2.2. Lagrangian formulation (LAG)

In order to model the chip formation (material separation from the workpiece to form the chip) and chip segmentation, a fracture-based model was used. This includes the fracture initiation/nucleation and fracture propagation/evolution.

A proper modeling of damage and fracture is essential and the corresponding models should consider both damage initiation, as well as damage evolution [5, 14]. In ductile materials, the damage initiation model should be established based on the material ductility, thus the equivalent strain at fracture. The latter is sensitive to the state of stress, being the stress triaxiality and the Lode angle two parameters that affect this strain [20, 21]. In the case of orthogonal cutting (plane-strain condition), the equivalent strain at facture is only affected by the stress triaxiality [14]. Increasing exigencies in terms of productivity leads to the application of high cutting speeds (High Speed Machining), and consequently the work material is submitted to high strain-rate levels. Therefore, the strain-rate sensitivity to fracture must be also included in the fracture model as well. Concerning to the temperature effects on the strain at fracture, what was mentioned above is also applied here. Therefore, a suitable model of fracture initiation in orthogonal metal cutting should consider both stress triaxiality and strain-rate effects. There are several fracture models that incorporate these effects, including the J-C ductile fracture model [11]. This model contains five failure parameters (D_1...D_5) and is usually represented by the following equation:

$$\bar{\varepsilon}_f = \left[D_1 + D_2 \cdot exp\left(D_3\eta\right)\right] \left[1 + D_4\,ln\left(\frac{\dot{\bar{\varepsilon}}}{\dot{\bar{\varepsilon}}_0}\right)\right] \left[1 + D_5\left(\frac{T - T_{room}}{T_m - T_{room}}\right)\right] \quad (2)$$

where $\bar{\varepsilon}_f$ is the equivalent fracture strain and $\eta = P/\bar{\sigma}$ is the stress triaxiality parameter. The determination of the five parameters (D_1...D_5) involves a series of experimental fracture tests, varying the stress triaxiality, strain-rate and temperature. Moreover, the implementation of such models in some FE codes can be a little more complex. For these reasons, in many metal cutting models, the fracture is ignored, because it is easier to model chip formation using non-physical criterion such as the remeshing procedure.

The fracture in a given finite element is initiated when a scalar damage parameter ω exceeds 1. This parameter is based on a cumulative law defined as:

$$\omega = \sum_{j=1}^{n} \left(\frac{\Delta \bar{\varepsilon}^{p}}{\bar{\varepsilon}_{0i}} \right)_j \quad (3)$$

Where $\Delta\bar{\varepsilon}^{p}$ is the increment of equivalent plastic strain during an increment of loading, j, in each integration point. The fracture evolution criterion is considered according to the published work referenced in [5].

Modelling of metal cutting process without a proper material constitutive model including fracture induces unrealistic material behaviour. Consequently, chip morphology (e.g., segmentation) obtained by such incomplete models produces an unrealistic tooth chip with unlimited material stretching and hardening [20].

2.3. Arbitrary Lagrangian - Eulerian formulation (ALE)

Because of the shortcomings of purely Lagrangian and purely Eulerian descriptions, a technique has been developed that succeeds, to a certain extent, in combining the best features of both the Lagrangian and the Eulerian approaches. Such a technique is known as the arbitrary Lagrangian-Eulerian (ALE) description. In the ALE description, the nodes of the computational mesh may be moved with the continuum in normal Lagrangian fashion, or be held fixed in Eulerian manner, or be moved in some arbitrary specified way to give a continuous rezoning capability. Because of this freedom in moving the computational mesh offered by the ALE description, greater distortions of the continuum can be handled than would be allowed by a purely Lagrangian method, with more resolution than that offered by a purely Eulerian approach. The mesh follows the boundary. However, this freedom in mesh movement has its limits. A treatment of mesh quality metrics and its limitations can be found in [22] and an extensive description of ALE methods can be found in [23].

2.4. Coupled Eulerian-Lagrangian formulation (CEL)

The coupled Eulerian-Lagrangian (CEL) formulation also attempts to capture the strengths of the Lagrangian and Eulerian formulations. In this paper, a Lagrangian is used to discretise the fixed structure (such as the cutting tool) while the Eulerian is used to discretize the fluid domain (such as the workpiece). The boundary of the Lagrangian domain is taken to represent the interface between the different domains [24]. Different CEL algorithms may be characterized by the details of how this interface condition is treated [25]. The general contact algorithm programmed in Abaqus/Explicit is adopted for the interface behaviour [26].

The elastic response of the work material has to be assumed to follow a linear elasticity model. The famous linear Mie-Gruneisen equation of state (EOS) can be employed. More detailed description of the EOS parameters can be referred to [27]. The corresponding parameters are given in Table. 3. The plastic behaviour follows the J-C constitutive model.

It's worth mentioning that both ALE and CEL formulations cannot model the fracture process, thus affecting the model's predictability.

3. Orthogonal cutting models of Ti-6Al-4V

3.1. Materials parameters and contact conditions

The physical properties of both work and tool materials, as well as the contact conditions are given in Table 1, whereas the J-C constitutive and fracture parameters of Ti–6Al–4V adopted in this study are given in Tables 2 and 3, which were obtained from experimental tests [31].

Table 1. Work and tool material properties and contact conditions [32, 33, 34]

Materials properties and contact conditions			
	Property	Workpiece	Tool
Materials	Density, ρ (*kg/m*^{3})	4430	15700
	Elastic modulus, *E* (*GPa*)	110	705
	Poisson's ratio, ν	0.33	0.23
	Specific heat, C_p (J/kg°C)	670	178
	Thermal conductivity, λ (W/m°C)	6.6	24.0
	Expansion coef., α_d (µm/m/°C)	9	5
	T_{melt} (°C)	1630	-
	T_{room} (°C)	25	
	Inelastic heat fraction, β	0.9	-
	Elastic bulk wave velocity, C_0 (*km/s*)	5.13	-
	Slop in v_s versus v_p diagram, *S*	1.028	-
	Grüneisen coefficient, γ_0	1.23	-
Contact	Heat transfer coefficient, *h* (*W/m*^{2} *K*)	4 x 10^4	
	Heat partition coefficient, α	0.5	
	Friction coefficient, μ	0.2	
	Friction energy transferred into heat, *E*	100 %	

In order to evaluate the influence of J-C constitutive model parameters on the cutting mechanics (cutting and thrust force - F_c and F_t, chip geometry, chip compression ratio - CCR and tool-chip contact length - l_c), two sets of J-C model parameters were used (Set-1 and Set 2).

Table 2. Johnson-Cook constitutive model parameters of Ti-6Al-4V [31].

Set	*A (MPa)*	*B (MPa)*	*n*	*C*	*m*	$\dot{\bar{\varepsilon}}_0$ (s^{-1})
J-C (set 1)	862	331	0.34	0.012	0.8	1
J-C (set 2)	1098	1092	0.93	0.014	1.1	1

Table 3. Johnson-Cook fracture model parameters of Ti-6Al-4V [31].

D_1	D_2	D_3	D_4	D_5	$\dot{\bar{\varepsilon}}_0$ (s^{-1})
-0.09	0.25	-0.5	0.014	3.87	1

3.2. Cutting conditions

The cutting parameters and tool geometry used in the simulation are listed in Table 4, where the uncoated cemented tungsten carbide cutting tool is used.

Table 4. Cutting parameters and tool geometry [18, 35].

Uncut chip thickness, t_1 (*mm*)	0.1
Cutting speed, v_c (*m/min*)	90
Rake angle, γ_n (deg)	0
Clearance angle, α_n (deg)	11
Width of cut, a_p (*mm*)	3
Cutting edge radius r_n (μm)	30

4. Simulation results and discussions

Three numerical models of orthogonal cutting were developed based on the three numerical formulations described in section 2. Fig. 1 shows the distribution of the equivalent plastic strain (PEEQ) for the three models, using the J-C parameters set 1. For the Lagrangian (LAG) model a high plastic strain is located in the chip side in contact with the tool rake face. However, both ALE and CEL models show higher plastic strain values at the machined surface when compared to the LAG one. This is due to the fact that the LAG model takes into accounts the work material damage and fracture to model technique applied to the predefined sacrificial layer. In order to avoid mesh distortion, the thickness of the sacrificial layer is considered to be of the same order of the cutting edge radius. In this case, the high sacrificial layer thickness when compared to the uncut chip thickness (30% of the uncut chip thickness) will affect the models predictions: lowering the plastic deformation in the machined surface, the chip thickness and the forces (see Table 5). On the contrary, the material damage and fracture are not taken into account in both the ALE and CEL models. Consequently, the stress increases permanently, leading to an increase in plastic strains, chip thickness and forces. It seems that using the J-C parameters set 1, ALE and CEL models present acceptable chip thickness when compared to the experimental value (Table 5).

As far as the J-C parameters set 2 is considered, Fig. 2 shows the distribution of the PEEQ for the three models. Using the LAG model, there is no obvious difference for both chip thickness, CCR and tool-chip contact length when compared to J-C parameters set 1. However, the J-C parameters set 2 induces greater forces when compared to the J-C parameters set 1. Using the ALE and CEL models, chip thickness, CCR and tool-chip and forces are greater for the J-C parameters set 2 when compared to the J-C parameters set 1. By the J-C parameters set 2, the best prediction concerning to cutting force was obtained by the LAG model.

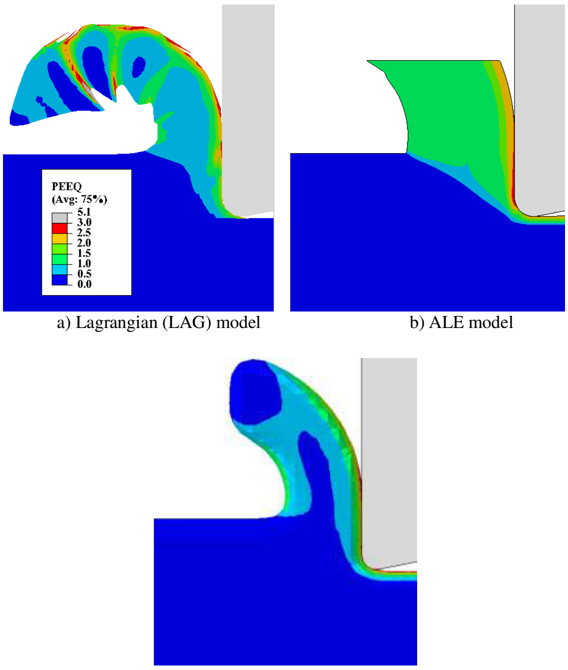

a) Lagrangian (LAG) model b) ALE model

c) CEL model

Fig. 1. Equivalent plastic strain distribution for J-C set 1.

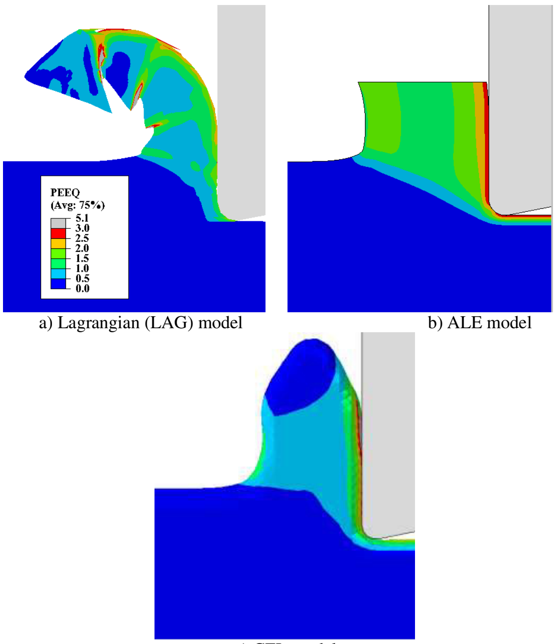

a) Lagrangian (LAG) model b) ALE model

c) CEL model

Fig. 2. Equivalent plastic strain distribution for J-C set 2.

Table 5. Measured (EXP) and predicted (SIM) results.

Parameter		Chip Peak (μm)	Chip Valley (μm)	Chip Pitch (μm)	l_c (mm)	CCR	F_c (N)	F_t (N)
EXP.		176	113	50.2	0.23 [(1)]	1.76	633	559
SIM J-C Set1	LAG	120	96	34.7	0.179	1.2	350	139
	ALE	169	-	-	0.140	1.69	485	255
	CEL	153	-	-	0.179	1.53	496	236
SIM J-C Set2	LAG	115	108	38.1	0.178	1.15	618	145
	ALE	223	-	-	0.201	2.23	948	297
	CEL	204	-	-	0.238	2.04	905	318

(1) Value calculated using the equation $l_c = t_1.CCR^{1.5}$ [37].

As far as the temperature distribution is concerned, it's worth mentioning that due to the short simulation time (0.4 ms for the three models) and eventually to low value of thermal conductance between the chip and tool used in the simulation, the steady-state thermal distribution was not reached for the three models [36]. However, this doesn't prevent to compare the temperatures between the two sets of J-C parameters, because the same cutting time was used in the three models for two sets J-C parameters.

As shown in Figs. 3 and 4, temperature distributions are different among the three models. The ALE and CEL models predict higher temperatures at tool-chip interface and machined surface when compared to the damage and fracture one. This can be also attributed to the damage and fracture used in the Lagrangian model not in the others two models.

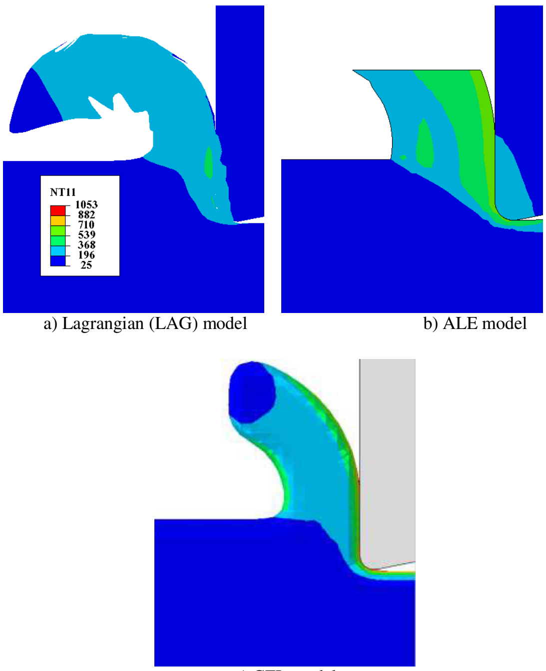

a) Lagrangian (LAG) model b) ALE model

c) CEL model

Fig. 3. Temperature distribution for J-C set 1.

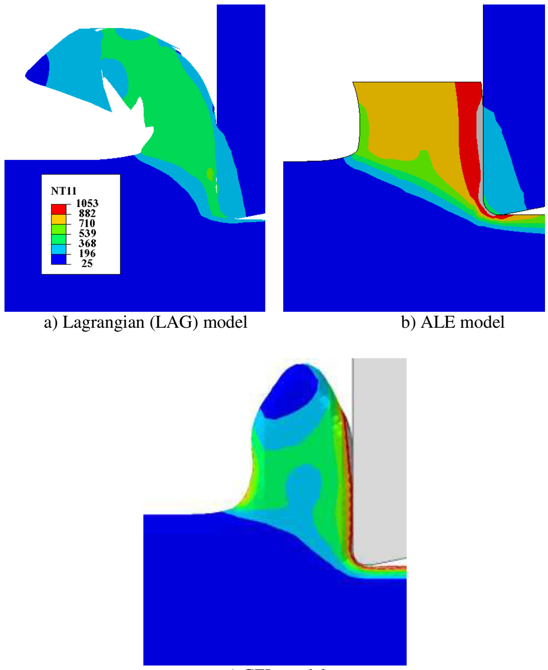

a) Lagrangian (LAG) model b) ALE model

c) CEL model

Fig. 4. Temperature distribution for J-C set2

The temperature distribution in the workpiece for ALE model is similar for both two J-C sets, while higher temperature is generated for J-C set 2. Do to the purely adiabatic calculation (the limitation of present Abaqus version, Abaqus 6.11) of the CEL model, high temperatures of 735° and 1259°C are observed at tool-chip interface (Fig.3(c) and Fig.4 (c)) when compared to those temperatures of LAG and ALE models, for both two J-C sets. The main reason is that the heat doesn't transfer to the cutting tool, which corresponds to no color plot in the cutting tool.

It should be mentioned that the J-C parameters related to the initial yield stress (A) and hardening part (B and n) directly determine the forces and influence the chip morphology.

5. Conclusion

Johnson-Cook constitutive model has been widely used in metal cutting simulations. Although this model is easy to apply and can describe the general response of work material deformation, it suffers from several drawbacks mentioned in section 1. Moreover, different sets of Johnson-Cook model parameters can be found in the literature, for the same work material. As it is frequently found in the literature [39, 40], if one wants to identify the most suitable set of Johnson-Cook model parameters, which produce the best fit between predicted and measured results, he or she usually needs to perform preliminary metal cutting simulations and compare the predicted results with those measured.

In this paper, an analysis of two sets of Johnson-Cook model parameters for Ti-6A-4V was performed, using three types of metal cutting models. Each model corresponded to a given numerical formulation: Lagrangian (LAG), Arbitrary Eulerian-Lagrangian (ALE) and Couple Lagrangian-Eulerian

(CEL). The results show that the set having lower hardening parameters (Set 1) gives acceptable chip thickness for the ALE and CEL models, while the set having higher hardening parameters (Set 2) presents good cutting force prediction for the LAG model. This means that, the best set of Johnson-Cook model parameters is not unique for the three numerical models of metal cutting. This is due to the fact that accuracy of the existing metal cutting models to predict the metal cutting performance does not depends only on the constitutive model, but also how these metal cutting models deal with the material separation from the workpiece to form the chip. This separation is tread differently in the three orthogonal cutting models presented in this contribution.

The differences between the LAG and ALE/CEL models are due to the fact that the damage model, which is used to produce chip formation and chip segmentation, is only supported in the LAG model. Unfortunately, the LAG model also suffers from two main drawbacks, which are the high mesh distortion and the material loss induced by the sacrificial layer [5]. These problems are minimized or avoided in the ALE and CEL models. Therefore, the selection of the most suitable set of Johnson-Cook model parameters from the literature, based on metal cutting numerical simulation and on the comparison between predicted and measured results is not the best practice.

Concerning to the Johnson-Cook constitutive model and their drawbacks related to the difficulties to reproduce the work material behaviour in metal cutting, this model should be replaced by other models, such us, those based on crystal plasticity theory [38].

References

[1] Outeiro J.C., Umbrello U, M'Saoubi R. Experimental and numerical modelling of the residual stresses induced in orthogonal cutting of AISI 316L steel. Int. J. Mach. Tools Manuf. 2006; 46 : 1786–1794.

[2] Umbrello D, Outeiro J.C., M'Saoubi R. The Influence of Johnson - Cook Material Constants on Finite Element Simulation of Machining of AISI 316L Steel. Int. J. Mach. Tools Manuf. 2007; 47: 462–470.

[3] Valiorgue F, Rech J, Hamdi H, Gilles P, Bergheau JM, A new approach for the modelling of residual stresses induced by turning of 316L. J. Mater. Process. Technol. 2007; 191: 270–273.

[4] Umbrello D, Outeiro J.C., M'Saoubi R, Jayal A, Jawahir IS. A numerical model incorporating the microstructure alteration for predicting residual stresses in hard machining of AISI 52100 steel, CIRP Ann. - Manuf. Technol. 2010; 59(1): 113–116.

[5] Mabrouki T, Girardin F, Asad M, Rigal JF. Numerical and experimental study of dry cutting for an aeronautic aluminium alloy (A2024-T351), Int. J. Mach. Tools Manuf. 2008; 48: 1187–1197.

[6] Altintas Y, Budak E. Analytical Prediction of Stability Lobes in Milling, CIRP Ann. - Manuf. Technol. 1995; 44: 357–362.

[7] Outeiro JC, Umbrello D, M'Saoubi R, Jawahir IS. Evaluation of Presente Numerical Models for Predicting Metal Cutting Performance and Residual Stresses. Mach. Sci. Technol.; 2015 (accepted for publication).

[8] Astakhov VP, Shvets S. The Assessment of Plastic Deformation in Metal Cutting. J. Mater. Process. Technol. 2004; 146: 193–202.

[9] Vaz Jr M, Owen DRJ, Kalhori V, Lundblad M, Lindgren LE. Modelling and simulation of machining processes. Arch. Comput. Methods Engng. 2007; 14(2): 173-204.

[10] Raczy A. , W. J. Altenhof, and A.T. Alpas. An Eulerian Finite element Model of the Metal Cutting Process. In: 8 th Internal LS-DYNA Users Conference: metal forming; 2004.

[11] Johnson GR, Cook WH. A constitutive model and data for metals subjected to large strains, high strain rates and high temperatures. In: Proc. 7th Int. Symp. On Ballistics, Hague, Netherlands, April 1983; 541–547.

[12] Guo YB, Wen Q, Horstemeyer MF. An internal state variable plasticity-based approach to determine dynamic loading history effects on material property in manufacturing processes, Int. J. Mech. Sci. 2005; 47: 1423–1441.

[13] Jawahir IS, Brinksmeier E, M'Saoubi R, Aspinwall DK, Outeiro JC, Meyer D, et al., Surface Integrity in Material Removal Processes: Recent Advances, CIRP Ann. - Manuf. Technol. Keynote Pap. 2011; 60: 603–626.

[14] Abushawashi Y, Xiao X., Astakhov V. FEM Simulation of Metal Cutting Using a New Approach to Model Chip Formation. Int. J. Adv. Mach. Form. Oper 2011; 3: 71–92.

[15] Kolsky H, An investigation of the material properties of materials at very high rates of loading, Proc Phy Soc B At. Mol. Phys. 1949; 62: 676–700.

[16] Jaspers S. Metal Cutting Mechanics and Material Behaviour. Ph.D, Technische Universiteit Eindhoven. 1999.

[17] Silva CMA, Rosa PA R, Martins PAF. Electromagnetic Cam Driven Compression Testing Equipment, Exp. Mech. 2012; 52: 1211–1222.

[18] Calamaz M, Coupard D and Girot F. A new material model for 2D numerical simulation of serrated chip formation when machining titanium alloy Ti-6Al-4V. Int. J. Mach. Tools Manuf. 2008; 48 (3-4): 275–288.

[19] Sima M and Ozel T. Modified material constitutive models for serrated chip formation simulations and experimental validation in machining of titanium alloy Ti-6Al-4V. Int. J. Mach. Tools Manuf. 2010; 50(11): 943–960.

[20] Abushawashi Y, Xiao X, Astakhov V. A novel approach for determining material constitutive parameters for a wide range of triaxiality under plane strain loading conditions. Int. J. Mech. Sci. 2013; 74: 133–142.

[21] Bai Y, Wierzbicki T. A new model of metal plasticity and fracture with pressure and Lode dependence, Int. J. Plast. 2008; 24: 1071–1096.

[22] Bijl H, van Zuijlen AH, de Boer A and Rixen DJ. Fluid-structure interaction. Delft institutes of aerospace and mechanical engineering, Delft; 2007.

[23] Done J, Huerta A, Ponthot JP and Rodríguez-Ferran A. Arbitrary Lagrangian-Eulerian methods, Encyclopedia of computational mechanics, Volume 1: fundamentals; 2004.

[24] Benson DJ. Computational methods in Lagrangian and Eulerian hydrocodes, Comp. Meth. Appl. Mech. Engng. 1992; 99: 235-394.

[25] Brown KH, Burns SP, and Christon MA. Coupled Eulerian-Lagrangian Methods for Earth Penetrating Weapon applications, U.S. Department of Commerce; 2002.

[26] ABAQUS, 'ABAQUS documentation', Dassault Systèmes, 2014.

[27] Wang XM and Shi J. Validation of Johnson-Cook plasticity and damage model using impact experiment. Int. J. Impact Eng. 2013; 60: 67-75.

[28] Notta-Cuvier D, Langrand B, Markiewicz E, Lauro F, and Portemont G. Identification of johnsoncook's viscoplastic model parameters using the virtual fields method: Application to titanium alloy Ti-6Al-4V. Strain 2013; 49: 22-45.

[29] Holmquist TJ and Johnson GR, Determination of constants and comparison of results for various constitutive models, Journal de Physique IV 1991; 01(C3): C3-853-C3-860.

[30] JUTRAS M. Improvement of the characterization method of the Johnson-cook model. Master thesis; 2008.

[31] Lesuer D R. Experiment investigations of material models for Ti–6Al–4V titanium and 2024-T3 Aluminum, Technical report; 2000.

[32] MATWEB. http://www.matweb.com, 2008.

[33] Wang YF and Yang ZG. A coupled finite element and meshfree analysis of erosive wear. Tribology international 2009; 42: 373-377.

[34] Zhang YC, Mabrouki T, Nelias D, Gong YD. Chip formation in orthogonal cutting considering interface limiting shear stress and damage evolution based on fracture energy approach. Finite Elem. Anal. Des. 2011; 47(7): 850-863.

[35] Zhang Y. Numerical simulation approaches and methodologies for multi-physic comprehensions of Titanium alloy (Ti–6Al–4V) cutting. PhD thesis, INSA de Lyon; 2011.

[36] Courbon C, Mabrouki T, Rech J, Mazuyer D, Perrard F, D'Eramo E. Further insight into the chip formation of ferritic-pearlitic steels: Microstructural evolutions and associated thermo-mechanical loadings. Int. J. Mach. Tools Manuf. 2014; 77: 34-46.

[37] V.P. Astakhov. Tribology of Metal Cutting. Elsevier; 2006.

[38] Zhang Y, Mabrouki T, Nelias D, Courbon C, Rech J, Gong Y. Cutting simulation capabilities based on crystal plasticity theory and discrete cohesive elements. J. Mater. Process Tech.2012; 212(4): 936-953.

[39] Pujana J, Arrazola PJ, MSaoubi R, Chandrasekaran H. Analysis of the inverse identification of constitutive equations applied in orthogonal cutting process. Int. J. Mach. Tools Manuf.2007; 47: 21532161.

[40] Asad M, Mabrouki T, Girardin F, Zhang Y, Rigal JF.Towards a physical comprehension of material strengthening factors during macro to micro-scale milling Mechanics 2011; 17(1): 97-104.